Preprints of the 21st IFAC World Congress (Virtual)
Berlin, Germany, July 12-17, 2020

Moving Area Tracking Formation Control of Multiple Autonomous Agents ⋆

Wenfei Zhang[1,2], **Yu Zhao**[1,2]

[1] Research and Development Institute of Northwestern Polytechnical University in Shenzhen, Shenzhen, 518057, China;

[2] School of Automation, Northwestern Polytechnical University, Xi'an, 710129, China (e-mail: yuzhao5977@gmail.com).

Abstract: This paper investigates a moving area tracking formation control (MATFC) problem of multiple autonomous agents, which aims at driving a group of agents to achieve a desired formation configuration and track a moving area. By using local information interaction among agents, a distributed MATFC protocol is proposed for single integrator dynamics. Without requiring the position and velocity of the center of the sub-area are bounded, the MATFC problem obtains greater application potential. During the moving process, the formation size can be regulated in real time to adapt the complicated environment through a scaling parameter. By adding a rotation matrix, the spatial orientation of each agent is capable of transforming in different cases. Then, based on the Lyapunov stability theory, it is verified that the objective of MATFC problem can be achieved under the proposed control protocol. Finally, numerical simulation results are shown to further demonstrate the effectiveness of the designed MATFC protocol.

Keywords: Multi-agent System, Moving Area Tracking Formation Control.

1. INTRODUCTION

In recent years, cooperative control problems of multi-agent systems, which exhibit coordination activities of multiple autonomous agents to accomplish the expected objective, have received great attention due to its wide range of applications, such as consensus (Liu et al. (2018)), distributed tracking (Zhao et al. (2013)), smart power grid (Zhang et al. (2014)), search and rescue (Baxter et al. (2007)), and environment monitoring (Vallejo et al. (2013)). As one of the most important research direction within the realm of multi-agent systems, formation control has been extensively investigated, which aims at driving a group of autonomous agents with local information interaction to achieve predefined formation configuration. In terms of the types of controlled variables, the existed work on formation control can be divided roughly into distance-based strategies and displacement-based strategies. In Bai et al. (2016), by utilizing the distance-based strategies, distance information among agents was actively controlled to achieve the expected formation. Although requiring relatively less information, some restrictions on the interaction topology of the multi-agent system were imposed. Then, in Meng et al. (2016), much richer formation patterns were achieved with using displacement-based strategies.

On the other hand, formation control can be classified into virtual structure, leader-follower, and behavior approaches. Based on virtual structure approach (Ren (2008)), entire formation of agents was regarded as a virtual rigid-body with the position of each agent relatively fixed. During the movement, the agents only needed to follow the predefined motions of corresponding virtual points. In leader-follower approach (Han et al. (2017)), several agents were selected as leaders and others were designated as followers. The followers transformed their states by means of exchanging information with the nearest leader. As for behavior approach in Lin et al. (2014), by coordinating some prescribed basic behaviors of multiple agents, the desired formation task was accomplished. In Ren (2007), three virtual structure, leader-follower, and behavior approaches were unified to the framework of consensus theory, furthermore, some consensus-based formation control protocols were proposed for second-order dynamics. And in Lin et al. (2016), the fixed formation control problem was studied by using the consensus-based approach. However, in order to address some requirements in actual application, such as target enclosing and obstacle avoidance, the configuration of formation should be variable. Thus, it is significant to consider the time-varying formation control problems. Since using the information of both formation configuration and its derivative, it brings greater difficulties and challenges than the fixed formation control problems. In He et al. (2019), considering the nonuniform communication delay, a distributed time-varying formation control algorithm was designed for second-order discrete multi-agent systems under switching topology.

However, in many practical cases such as moving target attacking and collaborative transportation, only achieving

⋆ This work was supported by the Science, Technology and Innovation Commission of Shenzhen Municipality under Grant JCYJ20190806151207250, the National Nature Science Foundation of China under Grant No. 61973252, and the China Postdoctoral Science Foundation under Grant No. 2018T111097.

the predefined formation configuration is far from enough, and the entire formation should also track the command trajectory determined by the real or virtual leader. Hence, Yang et al. (2018) studied the formation tracking problem for single integrator dynamics, where all agents can converge to the desired formation shape meanwhile maintaining its centroid tracking a given reference trajectory. In Dong and Hu (2017), based only local relative information, a time-varying formation tracking control algorithm was developed for linear multi-agent systems with a group of leaders, and the connection between the realizability of time-varying formation tracking and the dynamics of agents was revealed by using the properties of the Laplacian matrix. Then, in Hou et al. (2009), a dynamic region following formation control (DRFFC) problem was considered for a swarm of robots, where the shape of region is variable by means of selecting suitable functions, and multiple robots can form a dynamic formation without specific assignment of roles or orders in the formation. Further, utilizing relative position information among agents, Chen and Ren (2018) verified that distributed average tracking algorithms can be applied to solve the DRFFC problem, which can generate more abundant formation performance than before.

Inspired by the existing works, this paper focuses on the MATFC problem for single integrator dynamics. By designing distributed cooperative control protocol based on neighboring information interaction, multiple autonomous agents can track a specified moving area while keeping the predefined formation configuration. According to the actual mission requirement, the corresponding state trajectory of the center of moving area is determined to lead the entire formation to arrive at the object region. During the movement, the formation size is variable to overcome the disadvantage influence of geography environment, such as obstacle avoidance and tunnel crossing. Compared with the previous works in Chen and Ren (2018), the contribution of this paper mainly lies in the following two aspects. First, we remove the assumption required in Chen and Ren (2018) that the position and velocity of the center of the sub-area are bounded, which brings greater application value for MATFC problem. Specifically, in Chen and Ren (2018), the control gain is determined with the dynamic range of the center of the sub-area, which might lead to excessive redundancies. By using time-varying parameters design, the control gain can be adjusted in real time and appropriately. Second, by introducing a rotation matrix, each agent can rotate around the center of the formation to get their spatial redistribution without breaking the achieved formation configuration, which can obtain richer formation behavior. The formation with irregular shape can pass through a narrow tunnel more easily with its longest edge paralleled to the path through rotation. In addition, in view of the development prospect that a group of agents differ in function and carry respective parts based on task assignment, such as weapons, cameras, and radars only in few agents, the formation can adjust the spatial orientation of each agent to direct its functional region through the rotation, which contributes to rational utilization of the space and cost reduction.

The rest of this paper is organized as follows. In Section 2, the statement of MATFC problems and some useful lemmas are introduced. In Section 3, the design and analysis of distributed MATFC protocol are presented. Then, in Section 4, a numerical example is shown to demonstrate the obtained theoretical results. Finally, Section 5 gives the conclusion of the paper.

2. PROBLEM STATEMENT

In this paper, we consider a group of N agents on a graph $\mathcal{G}$. The dynamics of agent i is modeled by the following single integrator systems:

$$\dot{s}_i(t) = v_i(t), \quad i = 1, 2, \cdots, N, \tag{1}$$

where $s_i(t) \in \mathbb{R}^2$ and $v_i(t) \in \mathbb{R}^2$ represents the state and control input of agent i, respectively. An undirected graph $\mathcal{G}$ is defined by $\mathcal{G} = \{\mathcal{N}, \mathcal{E}\}$, where $\mathcal{N}$ is the set of nodes, and $\mathcal{E}$ is the set of edge. Let D denote the degree matrix of $\mathcal{G}$, A the adjacency matrix, B the incidence matrix, $L := D - A = BB^T$ the Laplacian matrix, and N_i the set of nodes which are connected to node i, which will be used in the text below.

Assumption 1. Graph $\mathcal{G}$ is undirected and connected.

As defined in Chen and Ren (2018), suppose that there is a group of targets, such as naval fleets and motorcades, which can be viewed as a whole in a moving area $R(t) \in \mathbb{R}^2$. Each target has its own sub-area $R_i(t) \subseteq R(t)$, whose dynamic information can be known for multiple agents respectively. The center of each sub-area $R_i(t)$ is defined as $r_i(t)$. As shown in Fig. 1, the whole area and sub-areas are severally indicated by the large ellipse and the smaller dotted circles. Generally, $r(t) = \frac{1}{N}\sum_{i=1}^{N} r_i(t)$ can be regarded as an estimation of the center of the moving area $R(t)$. If consider multiple independent target tracking subproblems only, agents can not achieve the desired formation, which is adverse to the collaboration among agents. The MATFC problem aims at driving multiple agents to track the moving area while maintaining the desired formation.

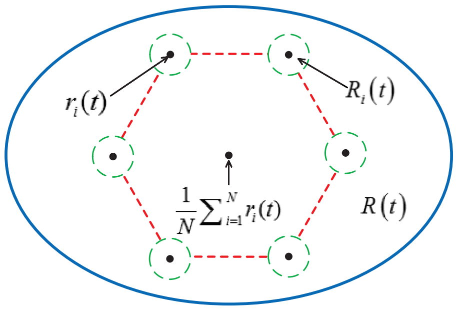

Fig. 1. Illustration of the moving area.

The desired formation configure is determined by $s_i - s_j = \tilde{h}_{ij} = \frac{1}{g(t)} M h_{ij}$, $(i,j) \in \mathcal{E}$, where $h_{ij} = h_i - h_j$ are constants specifying the relative displacement between the agents, $0 < \underline{g} \le g(t) \le \overline{g} < +\infty$ is a scaling parameter used to regulate the size of the formation to overcome some unfavorable environmental factors, and M is a rotation matrix to adjust the spatial orientation of each agent, which is defined as

$$M = \begin{pmatrix} \cos\theta & \sin\theta \\ -\sin\theta & \cos\theta \end{pmatrix}. \tag{2}$$

The rotation angle satisfies $\theta = \omega(t - t_0) + \phi$, where ω denotes angular velocity, t_0 start time, and ϕ initial angle of rotation. Note that $M^{-1} = M^T$, which can be viewed as the rotation in opposite direction. It is believed that the desired formation is achieved when the following equation is established:

$$\lim_{t\to\infty} \left\| s_i(t) - s_j(t) - G^{-1}(t)(h_i - h_j) \right\| = 0, \qquad (3)$$

where $G(t) = g(t)M^T$, and $s_i(t) - s_j(t) - G^{-1}(t)(h_i - h_j) = \xi_{ij}(t)$ can be viewed as the formation error. Because all agents must be able to enter into the moving area, it is necessary to require that

$$\frac{1}{N}\sum\nolimits_{i=1}^{N} r_i(t) + G^{-1}(t)h_i \in R(t). \qquad (4)$$

If each agent eventually trace into the moving area, we have

$$\lim_{t\to\infty} \left\| s_i(t) - \frac{1}{N}\sum\nolimits_{i=1}^{N} r_i(t) - G^{-1}(t)h_i \right\| = 0, \qquad (5)$$

where $s_i(t) - \frac{1}{N}\sum_{i=1}^{N} r_i(t) - G^{-1}(t)h_i = \eta_i(t)$ is defined as the tracking error.

Remark 1. Different from the DRFFC problem in Hou et al. (2009), the shape of the moving area is not described by certain functions, and has no effect on the realization of the control objects (3) and (5). In case of scaling and rotation, the condition (4) can guarantee that the moving area is large enough to contain the obtained formation.

Remark 2. Note that (3) can be got from (5), which reflects the whole-part relationship in the course of solving the MATFC problem. Indicated by (3) directly, multiple agents achieve the desired formation firstly, and then the center of the formation tracks the center of the moving area, which leads to (5). The following proof will be presented according this process similarly.

Now we get ready to provide the definition of moving area tracking formation control problem.

Definition 1. For multi-agent system (1), by designing a distributed control protocol $u_i(t)$, the desired formation configuration and area tracking is finally achieved if (3) and (5) are satisfied. In other words, both the formation error $\xi_i(t)$ and the tracking error $\eta_i(t)$ converge to zero as $t \to \infty$.

Some useful lemmas are given to facilitate the following analysis.

Lemma 1. (Godsil and Royle (2001)) Under Assumption 1, zero is a simple eigenvalue of L with $\mathbf{1}$ as its associated eigenvector and all the other eigenvalues are positive. Furthermore, the smallest nonzero eigenvalue λ_2 of L satisfies $\lambda_2 = \min\limits_{x\neq 0, \mathbf{1}^T x = 0} \frac{x^T L x}{x^T x}$.

Lemma 2. (Ghapani et al. (2019)) Under Assumption 1, for any vector $z \in R^n$, one gets $z^T LBH\text{sgn}(B^T z) \geq \lambda_2 z^T BH\text{sgn}(B^T z)$, where H is a positive-definite diagonal matrix, $\text{sgn}(B^T z)$ is the sign function.

3. MAIN RESULTS

Consider the following MATFC protocol for system (1):

$$\begin{aligned} v_i(t) = & -G^{-1}(t)\dot{G}(t)(s_i(t) - r_i(t)) + \dot{r}_i(t) \\ & - \left(s_i(t) - r_i(t) - G^{-1}(t)h_i\right) \\ & - \sum_{j\in N_i} \rho_{ij}\text{sgn}\Big[s_i(t) - s_j(t) \\ & -G^{-1}(t)(h_i - h_j)\Big], \end{aligned} \qquad (6)$$

where $\rho_{ij} = \mu\left(\left\|\sigma_i(t)\right\| + \left\|\sigma_j(t)\right\| + \left\|\dot{\sigma}_i(t)\right\| + \left\|\dot{\sigma}_j(t)\right\|\right) + \gamma = \mu c_{ij} + \gamma$, represent time-varying parameters based on the state of agent i and its neighbor agent j, $\sigma_i(t) = G(t)r_i(t)$, and μ, γ are positive constants, respectively.

Remark 3. As an extension of the approach in Chen and Ren (2018), the state-dependent time-varying parameter instead of a constant control gain is used to offset the effect from the dynamic of the sub-areas, and a rotation matrix is introduced to enrich the formation behavior, which both of them make the controller design and stability analysis more difficult.

Theorem 1. For single-integrator system (1), the control objective of MATFC problem can be achieved using the designed MATFC protocol (6) if Assumption 1 is satisfied, $\mu > \frac{1}{\underline{g}\lambda_2(L)}$, and $\gamma > 0$.

Proof: First, in order to demonstrate the desired formation is obtained, i.e., $\lim\limits_{t\to\infty} \Big\| s_i(t) - s_j(t) - G^{-1}(t)(h_i - h_j) \Big\| = 0$, we provide an auxiliary variable $\zeta_i(t) = G(t)s_i(t) - h_i$ and take the derivative of $\zeta_i(t)$, which yields

$$\begin{aligned} \dot{\zeta}_i(t) = & \dot{G}(t)s_i(t) + G(t)\dot{s}_i(t) \\ = & \dot{G}(t)s_i(t) + G(t)v_i(t) \\ = & \dot{G}(t)r_i(t) + G(t)\dot{r}_i(t) + G(t)r_i(t) \\ & -\zeta_i(t) - G(t)\sum_{j\in N_i}\rho_{ij}\text{sgn}\left[G^{-1}(t)\right. \\ & \left.(\zeta_i(t) - \zeta_j(t))\right] \\ = & \dot{\sigma}_i(t) + \sigma_i(t) - \zeta_i(t) \\ & - \sum_{j\in N_i} g(t)M^T\rho_{ij}\text{sgn}\left[M(\zeta_i(t) - \zeta_j(t))\right]. \end{aligned} \qquad (7)$$

The last step follows from $\text{sgn}[G^{-1}(t)(\zeta_i(t) - \zeta_j(t))] = \text{sgn}\left[\frac{1}{g(t)}M(\zeta_i(t) - \zeta_j(t))\right] = \text{sgn}\left[M(\zeta_i(t) - \zeta_j(t))\right]$ for any $g(t) \geq \underline{g} > 0$. Let $\otimes$ denote the Kronecker product, $\zeta = [\zeta_1^T, \zeta_2^T, \cdots, \zeta_N^T]^T$, $\sigma = [\sigma_1^T, \sigma_2^T, \cdots, \sigma_N^T]^T$, $H = \text{diag}(\rho_{ij})$. Next, (7) can be rewritten in matrix form, one has

$$\begin{aligned} \dot{\zeta}(t) = & \dot{\sigma}(t) + \sigma(t) - \zeta(t) \\ & -g(t)(BH \otimes M^T)\text{sgn}[(B^T \otimes M)\zeta(t)]. \end{aligned} \qquad (8)$$

Denoting $P = I_N - \frac{\mathbf{1}\mathbf{1}^\mathbf{T}}{N}$, where I_N is the N-dimensional identity matrix, and $\mathbf{1}$ is the vector with all ones, one obtains $PB = BP = B$. Hence, multiply both sides of (8) by $P \otimes I_2$ and let $Z(t) = [Z_1^T, Z_2^T, \cdots, Z_N^T]^T = (P \otimes I_2)\zeta(t)$. It follows that

$$\begin{aligned} \dot{Z}(t) = & (P \otimes I_2)\dot{\sigma}(t) + (P \otimes I_2)\sigma(t) - Z(t) \\ & -g(t)(BH \otimes M^T)\text{sgn}[(B^T \otimes M)Z(t)]. \end{aligned} \qquad (9)$$

Consider the following Lyapunov function:

$$V(t) = \frac{1}{2} Z^T(t)(L \otimes I_2)Z(t). \tag{10}$$

Using the fact that $(\mathbf{1}^T \otimes I_2)Z(t) = 0$, one has

$$V(t) \geq \frac{\lambda_2(L)}{2} Z^T(t)Z(t). \tag{11}$$

Then, taking the time derivative of (10) along (9), one gets

$$\begin{aligned}\dot{V}(t) &= Z^T(t)(L \otimes I_2)\dot{Z}(t) \\ &= Z^T(t)(L \otimes I_2)\dot{\sigma}(t) + Z^T(t)(L \otimes I_2)\sigma(t) \\ &\quad - Z^T(t)(L \otimes I_2)Z(t) \\ &\quad - g(t)Z^T(t)(LBH \otimes M^T)\mathrm{sgn}[(B^T \otimes M)Z(t)].\end{aligned} \tag{12}$$

Denote $\bar{L} = B^T B$. Because L and $\bar{L}$ have the same nonzero eigenvalues, it follows from Lemma 2 that

$$\begin{aligned}&-g(t)Z^T(t)(LBH \otimes M^T)\mathrm{sgn}[(B^T \otimes M)Z(t)] \\ &= -g(t)[(B^T \otimes M)Z(t)]^T(\bar{L}H \otimes I_2) \\ &\quad \mathrm{sgn}[(B^T \otimes M)Z(t)] \\ &\leq -g(t)\lambda_2(L)[(B^T \otimes M)Z(t)]^T(H \otimes I_2) \\ &\quad \mathrm{sgn}[(B^T \otimes M)Z(t)] \\ &\leq -g(t)\lambda_2(L)\sum_{i=1}^{N}\sum_{j\in\mathcal{N}_i}\rho_{ij}\left\| M\left[Z_i(t) - Z_j(t)\right]\right\| \\ &\leq -\underline{g}\lambda_2(L)\sum_{i=1}^{N}\sum_{j\in\mathcal{N}_i}(\mu c_{ij} + \gamma)\left\|Z_i(t) - Z_j(t)\right\|.\end{aligned} \tag{13}$$

The above can be verified from $\|M\left(Z_i\left(t\right) - Z_i\left(t\right)\right)\| = \left\|\begin{pmatrix}\cos\theta & \sin\theta \\ -\sin\theta & \cos\theta\end{pmatrix}\left(Z_i\left(t\right) - Z_i\left(t\right)\right)\right\| = \|Z_i\left(t\right) - Z_j\left(t\right)\|$. On the other hand, we have

$$\begin{aligned}&Z^T(t)(L \otimes I_2)\dot{\sigma}(t) + Z^T(t)(L \otimes I_2)\sigma(t) \\ &= \sum_{i=1}^{N}(\sigma_i(t) + \dot{\sigma}_i(t))\sum_{j\in\mathcal{N}_i}(Z_i(t) - Z_j(t)) \\ &\leq \sum_{i=1}^{N}(\|\sigma_i(t)\| + \|\dot{\sigma}_i(t)\|)\sum_{j\in\mathcal{N}_i}\|Z_i(t) - Z_j(t)\| \\ &\leq \sum_{i=1}^{N}\sum_{j\in N_i}c_{ij}\left\|Z_i\left(t\right) - Z_j\left(t\right)\right\|,\end{aligned} \tag{14}$$

where $c_{ij} = \left\|\sigma_i\left(t\right)\right\| + \left\|\sigma_j\left(t\right)\right\| + \left\|\dot{\sigma}_i\left(t\right)\right\| + \left\|\dot{\sigma}_j\left(t\right)\right\|$. Substituting (13) and (14) into (12), one has

$$\begin{aligned}\dot{V}\left(t\right) \leq& -Z^T\left(t\right)\left(L \otimes I_2\right)Z\left(t\right) - \sum_{i=1}^{N}\sum_{j\in N_i}\Big[\big(\mu\underline{g}\lambda_2\left(L\right) \\ &-1\big)c_{ij} + \gamma\lambda_2\left(L\right)\Big]\left\|Z_i\left(t\right) - Z_j\left(t\right)\right\|.\end{aligned} \tag{15}$$

Since $c_{ij} \geq 0$, by choosing $\mu > \frac{1}{\underline{g}\lambda_2(L)}$ and $\gamma > 0$, one has

$$\begin{aligned}\dot{V}(t) &\leq -Z^T(t)(L \otimes I_2)Z(t) \\ &\leq -\lambda_2(L)Z^T(t)Z(t) \\ &< 0.\end{aligned} \tag{16}$$

Thus, $\lim_{t\to\infty}\|Z_i(t)\| = 0$, which implies $\lim_{t\to\infty}\|\zeta_i - \zeta_j\| = 0$. Then, one obtains $\lim_{t\to\infty}\left\|s_i\left(t\right) - s_j\left(t\right) - G^{-1}\left(t\right)\left(h_i - h_j\right)\right\| = 0$.

Next, note that $Z(t) = (P \otimes I_2)\zeta(t)$, which yields $\lim_{t\to\infty}\left\|\zeta_i - \frac{1}{N}\sum_{j=1}^{N}\zeta_j\right\| = 0$. Let $\Phi = \frac{1}{N}\sum_{i=1}^{N}(\zeta_i(t) - \sigma_i(t))$. Then, it follows from (7) that

$$\begin{aligned}\dot{\Phi} &= -\Phi - \frac{1}{N}\sum_{i=1}^{N}\sum_{j\in\mathcal{N}_i}G(t)\rho_{ij}\mathrm{sgn}\left[G^{-1}\left(t\right)\left(\zeta_i(t) - \zeta_j(t)\right)\right] \\ &= -\Phi.\end{aligned} \tag{17}$$

Hence, one has $\lim_{t\to\infty}\|\Phi\| = \lim_{t\to\infty}\left\|\frac{\sum_{i=1}^{N}(\zeta_i(t) - \sigma_i(t))}{N}\right\| = 0$. Then, $\lim_{t\to\infty}\left\|\zeta_i\left(t\right) - \frac{1}{N}\sum_{i=1}^{N}\sigma_i\left(t\right)\right\| = \lim_{t\to\infty}\Big\|G\left(t\right)s_i\left(t\right) - h_i - \frac{1}{N}\sum_{i=1}^{N}G\left(t\right)r_i\left(t\right)\Big\| = 0$. Noting that $G(t) = g(t)M^T, g(t) \geq \underline{g} > 0$, one has $\lim_{t\to\infty}\Big\|s_i\left(t\right) - \Big[\frac{1}{N}\sum_{i=1}^{N}r_i\left(t\right) + G^{-1}\left(t\right)h_i\Big]\Big\| = 0$. This completes the proof.

Remark 4. Compared with the previous works in Chen and Ren (2018), we do not require that $r_i(t)$ and $\dot{r}_i(t)$ are bounded in this paper, which expands the range of applications and development prospect for MATFC problem. At an additional price, the information of $r_i\left(t\right), \dot{r}_i\left(t\right), r_j\left(t\right), \dot{r}_j\left(t\right)$ is used to determine the time-varying parameter, which brings the greater burden of computation and communication.

Remark 5. Specially, when $\mu = 0$, the control objective of MATFC problem can also be achieved with bounded $\sigma_i(t), \dot{\sigma}_i(t)$, if $\gamma > \frac{\|\sigma_i(t)\| + \|\dot{\sigma}_i(t)\|}{\underline{g}\lambda_2(L)}$. Thus, the proposed MATFC protocol (6) can also apply to the related DRFFC problem investigated in Chen and Ren (2018) rather than the contrary.

4. SIMULATIONS

The effectiveness of the proposed MATFC protocol is illustrated through a numerical example in this section. Consider a single integrator multi-agent system of six agents, where the initial states of all agents are generated randomly. The undirected interaction topology is shown in Fig. 2. As shown in Fig. 3, the centers of the six sub-areas are desired by $r_i\left(t\right) = \left[2.5t + 5 + \left(-1\right)^i\left|i - 3.5\right|\sin t; 20 + \left(-1\right)^i\left|i - 3.5\right|\sin t\right]$, $i = 1, 2, ..., 6$, and then the center of the moving area is $r(t) = [2.5t + 5; 20]$, which implies the area moves horizontally to the right. The formation constant vector is given by $h = [{h_1}^T, {h_2}^T, {h_3}^T, {h_4}^T, {h_5}^T, {h_6}^T]^T = [4, 0, 2, -3, -2, -3, -4, 0, -2, 3, 2, 3]^T$. To regulate the size of the formation, the time-varying scaling parameter is presented as the following:

$$g(t) = \begin{cases} 1 & t \in [0, 2) \cup [8, 12) \\ 1 + 3 \times \dfrac{t-2}{2} & t \in [2, 4) \\ 4 & t \in [4, 6) \\ 1 + 3 \times \dfrac{8-t}{2} & t \in [6, 8). \end{cases} \tag{18}$$

For the rotation angle $\theta = \omega(t - t_0) + \phi$, we choose

$$\omega = \begin{cases} 0 & t \in [0, 8) \cup [10, 12) \\ 1.45\pi & t \in [8, 10), \end{cases} \tag{19}$$

and

$$\phi = \begin{cases} 0 & t \in [0, 10) \\ 0.9\pi & t \in [10, 12). \end{cases} \tag{20}$$

In Fig. 4, the big green ellipse indicates the moving area, each small square represents an agent, the small hollow pentagram denotes a special agent with different function modules, such as cameras, radars, and weapons. The target is marked by red solid pentagram, which required the surveillance or attacking of the formation. Two fold lines make up a exit door which needs all agents to pass through. Fig. 4(a) shows the initial position of each agent. In Fig. 4(b), we observe that the desired formation is achieved and the moving area is tracked for all agents. From Fig. 4(c), the formation is regulating its size to adapt the width of the exit door. Then in Fig. 4(d), the formation has shrunk to $\frac{1}{4}$ size as before. As arrived outside the exit door, the formation size is restored in Fig. 4(e). Fig. 4(f) show that the specific agent turns toward the target through the rotation of the formation. The corresponding state trajectories of six agents within time $T = 12$s are given in Fig. 5. It is worth mentioning that the desired formation can not be obtained if each agent only tracks the center of its corresponding sun-area.

In the following, the time-varying curves of the formation errors $\xi_{ij}(t)$ and the tracking errors $\eta_i(t)$ are shown, where superscript (1) and (2) represent the first and second element of errors, respectively. In Fig. 6, we can see the formation error converge to zero, which implies the desired formation is achieved. And in Fig. 7, the tracking error also converge to zero, which means that the formation enters into and tracks the moving area. Therefore, the objective of MATFC problem is obtained. As shown in Fig. 8, using the non-smooth signum function in the proposed algorithm causes the control chattering, which is necessary to be extended to a continuous MATFC algorithm to get better application performance in the future.

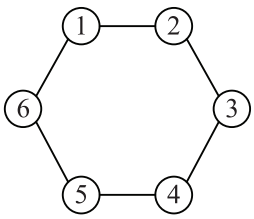

Fig. 2. Interaction topology for six agents.

5. CONCLUSIONS

In this paper, a MATFC problem for single integrator multi-agent system has been considered. Without requiring the position and velocity of the center of the sub-area are bounded, the MATFC problem can be applied to more practical cases. By using a time-varying scaling parameter, the formation size is adjustable in real time to avoid obstacle. The flexibility of the formation has also been extended by introducing a rotation matrix, which contributes to functional coordination and complementarity

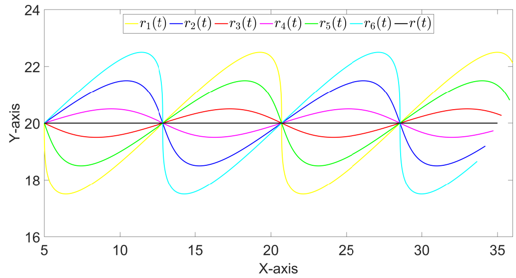

Fig. 3. The state trajectories of the center of multiple sub-areas and the whole moving area.

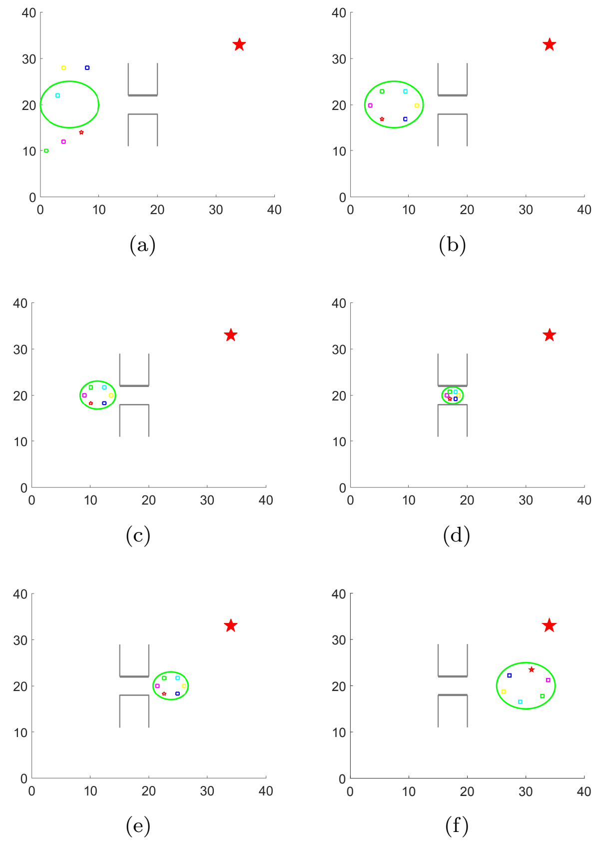

Fig. 4. Positions of six agents at times: (a) $t = 0$s; (b) $t = 1$s; (c) $t = 2.5$s: (d) $t = 5$s; (e) $t = 7.5$s; (f) $t = 10$s. Each small square and hollow pentagram is an agent. The large ellipse represent a moving area. Two fold lines constitute an assumed exit door. The red solid pentagram denotes a target.

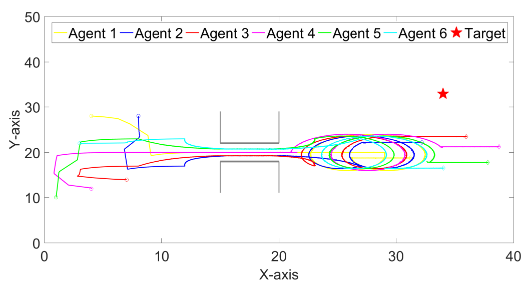

Fig. 5. State trajectories of six agents.

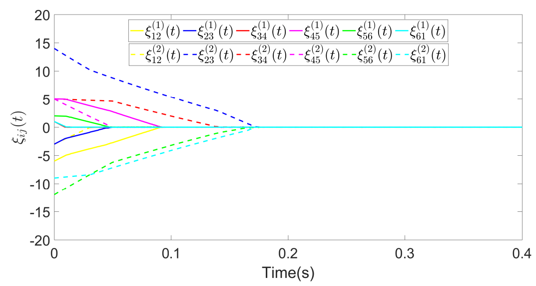

Fig. 6. The formation errors $\xi_{ij}(t)$.

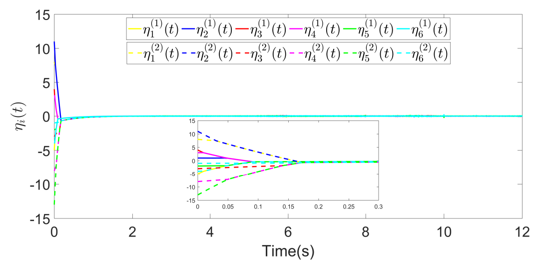

Fig. 7. The tracking errors $\eta_i(t)$.

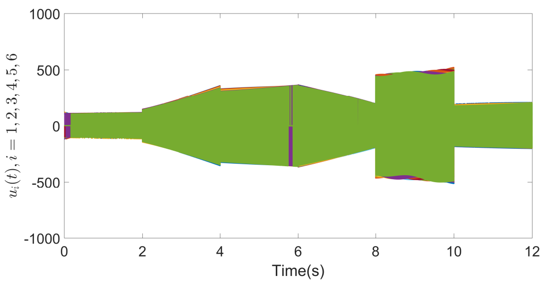

Fig. 8. Control inputs of the MATFC algorithm.

among agents. The effectiveness of the designed MATFC protocol has been verified by numerical simulation.

In the future, noting the eigenvalue of Laplacian matrix is used in the proposed MATFC protocol, a fully distributed adaptive MATFC problem is worthy of study to remove the global information. In addition, the MATFC problem can be extended to the directed graph, and nonlinear system.

REFERENCES

Liu, Y.F., Zhao, Y., Ren, W., and Chen, G.R. (2018). Appointed-time consensus: Accurate and practical designs. *Automatica*, 89, 425–429.

Zhao, Y., Duan, Z.S., Wen, G.H., and Zhang, Y.J. (2013). Distributed finite-time tracking control for multi-agent systems: An observer-based approach. *Systems & Control Letters*, 62(1), 22–28.

Zhang, W., Liu, W.X., Wang, X., Liu, L.M., and Ferrese, F. (2014). Distributed multiple agent system based online optimal reactive power control for smart grids. *IEEE Transactions on Smart Grid*, 5(5), 2421–2431.

Baxter, J.L., Burke, E.K., Garibaldi, J.M., and Norman, M. (2007). Multi-robot search and rescue: a potential field based approach. *Autonomous Robots and Agents*, 76, 19–16.

Vallejo, D., Villanueva, F.J., Garca, L.M., Gonzalez, C., and Albusac, J. (2013). An agent-based approach to understand events in surveillance environments. *2013 IEEE/WIC/ACM International Joint Conferences on Web Intelligence (WI) and Intelligent Agent Technologies (IAT), Atlanta, GA*, 100–103.

Bai, L., Chen, F., and Lan, W.Y. (2016). Distributed tracking of a non-minimally rigid formation for multi-agent systems. *International Journal of Systems Science*, 48(1), 161–170.

Meng, Z.Y., Anderson, B.D.O., and Hirche, S. (2016). Formation control with mismatched compasses. *Automatica*, 69, 232–241.

Ren, W. (2008). Decentralization of virtual structures in formation control of multiple vehicle systems via consensus strategies. *European Journal of Control*, 14(2), 93–103.

Han, T., Guan, Z.H., Chi, M., Hu, B., Li, T., and Zhang, X.H. (2017). Multi-formation control of nonlinear leader-following multi-agent systems. *ISA Transactions*, 69, 140–147.

Lin, J.L., Hwang, K.S., and Wang, Y.L. (2014). A simple scheme for formation control based on weighted behavior learning. *IEEE Transactions on Neural Networks and Learning Systems*, 25(6), 1033–1044.

Ren, W. (2007). Consensus strategies for cooperative control of vehicle formations. *IET Control Theory & Applications*, 1(2), 505–512.

Lin, Z.Y., Wang, L.L., Han, Z.M., and Fu, M.Y. (2016). A graph Laplacian approach to coordinate-free formation stabilization for directed networks. *IEEE Transactions on Automatic Control*, 61(5), 1269–1280.

He, L.L., Zhang, J.Q., Hou, Y.Q., Liang, X.L., and Bai, P. (2019). Time-varying formation control for second-order discrete-time multi-agent systems with switching topologies and nonuniform communication delays. *IEEE Access*, 7, 65379–65389.

Yang, Q.K., Cao, M., Marina, H.G., Fang, H., and Chen, J. (2018). Distributed formation tracking using local coordinate systems. *Systems & Control Letters*, 111, 70–78.

Dong, X.W. and Hu, G.Q. (2017). Time-varying formation tracking for linear multiagent systems with multiple leaders. *IEEE Transactions on Automatic Control*, 62(7), 3658–3664.

Hou, S.P., Cheah, C.C., and Slotine, J.J.E. (2009). Dynamic region following formation control for a swarm of robots. *2009 IEEE International Conference on Robotics and Automation, Kobe*, 1929–1934.

Chen, F. and Ren, W. (2018). A connection between dynamic region-following formation control and distributed average tracking. *IEEE Transactions on Cybernetics*, 48(6), 1760–1772.

Godsil, C. and Royle G. (2001). Algebraic graph theory. *New York, NY, USA: Springer.*

Ghapani, S., Rahili, S., and Ren, W. (2019). Distributed average tracking of physical second-order agents with heterogeneous unknown nonlinear dynamics without constraint on input signals. *IEEE Transactions on Automatic Control*, 3(64): 1178–1184.